Rheological Properties of Branched Low-Density Polyethylene

CHANG DAE HAN, YONG JOO KIM, HSIAO-KEN CHUANG, and TAE HOON KWACK, *Department of Chemical Engineering, Polytechnic Institute of New York, Brooklyn, New York 11201*

Synopsis

The shear flow properties of six commercially available long-chain branching low-density polyethylene resins were determined, using a cone-and-plate rheometer at *low* shear rates and a capillary rheometer at *high* shear rates. Also determined were the elongational viscosities of the resins, using an apparatus developed by Ide and White. Interpretation of the rheological measurements is given with the aid of the molecular parameters, namely, molecular weight and molecular weight distribution.

INTRODUCTION

Low-density polethylene is, among all polyolefins, one of the resins in greatest demand in industrial consumption. Its use includes such applications as wire coating, film extrusion, foam extrusion, etc. A variety of grades are available from resin manufacturers. Each grade is aimed at specific processing applications, requiring certain desired flow characteristics as well as certain physical/mechanical properties in the final products.

It is important to control the rheological properties of the resin, which are intimately related to the molecular parameters, i.e., molecular weight (MW) and molecular weight distribution (MWD). In dealing with low-density polyethylene (LDPE), an additional molecular parameter, long-chain branching (LCB), is believed to play an important role in its rheological behavior. In the past, some investigators[1–5] have studied the effect of MW and MWD and, also, the effect of the amount of LCB on the rheological properties of LDPE.

From the processing point of view, it is important to determine the rheological properties experimentally. This is especially desirable for the elastic property of a bulk polymer in the molten state at *high* shear rates or stresses. It should be noted that many polymers of industrial importance, certainly LDPE, exhibit nonlinear behavior in their viscous and elastic properties under practical processing conditions, i.e., at high shear rates or stresses. Therefore, any attempt to extrapolate the rheological data obtained at *low* shear rates to that at *high* shear rates requires extreme caution, to say the least. It is a common practice today to use a cone-and-plate rheometer (e.g., Weissenberg rheogoniometer; Rheometrics Mechanical Spectrometer) for determining the shear flow properties (viscosity and normal stress differences) of molten polymers at *low* shear rates (say, below 10 s^{-1}), and a plunger-type viscometer (e.g., Instron viscometer) in determining the melt viscosity at *high* shear rates. Since the shear rates encountered in almost all commercial polymer processing operations are high (say,

Journal of Applied Polymer Science, Vol. 28, 3435–3451 (1983)
 CCC 0021-8995/83/113435-17$02.70

TABLE I
Summary of Molecular Parameters of the Branched LDPE's Employed

Sample code	$\bar{M}_n \times 10^{-4}$	$\bar{M}_w \times 10^{-5}$	$\bar{M}_w/\bar{M}_n$	Melt index
Dow 510	1.39	1.12	8.1	2.0
Dow 529	0.94	0.86	9.1	2.0
Norchem 952	2.02	3.70	18.3	2.0
Norchem 962	2.24	3.98	17.8	1.0
Rexene 111	1.70	1.35	7.9	5.5
Rexene 143	2.00	1.41	7.0	5.0

100–1,000 s^{-1}), the rheological properties determined by a cone-and-plate rheometer at *low* shear rates are of little practical value for predicting the rheological properties of thermoplastic molten polymers at commercially useful shear rates. On the other hand, the plunger-type viscometer that makes use of force measurements of the descending plunger *cannot* provide information on the elastic property of molten polymers. Measurements of extrudate swell ratio d_j/D (where d_j is the completely relaxed extrudate diameter and D is the capillary diameter) from a capillary must not be used for calculating the first normal stress difference $\tau_{11} - \tau_{22}$, because accurate measurements of d_j/D that are, for instance, free of the gravitational effect are extremely difficult, if not impossible, to obtain.

It is a well-accepted fact today, in many polymer processing operations, that one must bring under control the elastic property of a polymer in order to have consistent quality of products. Hence, it is essential for one to measure the elastic property of molten polymers at the same high shear rates or stresses that one would find in commercial operations.

As part of our continuing effort in establishing relationships between the molecular parameters of polymers and their rheological properties, we very recently conducted an experimental investigation of the influence of molecular

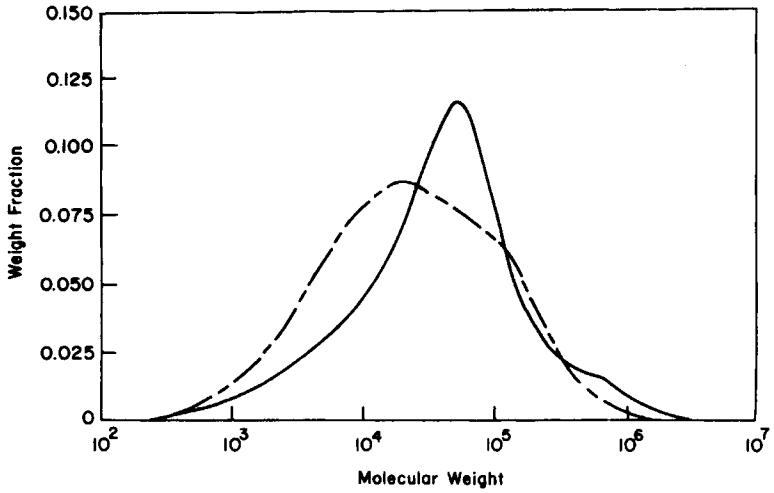

Fig. 1. Molecular weight distribution curves for Dow Chemical low-density polyethylenes: (—) PE510; (- - -) PE529.

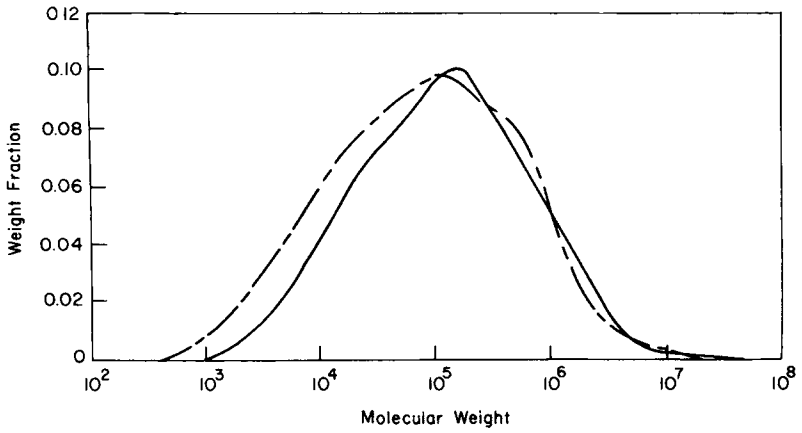

Fig. 2. Molecular weight distribution curves for Northern Petrochemicals low-density polyethylenes: (—) PE952; (- - -) PE962.

weight distribution on the rheological properties of branched (high-pressure) low-density polyethylene. Special attention was paid to determining the elastic property of the resin at high shear rates.

EXPERIMENTAL

Materials

Six different grades of commercially available long-chain branching low-density polyethylene (LDPE) were used in our study. Specifically, we have chosen two different grades of LDPE from each of these manufacturers, as shown in Table I. The molecular weights of these resins were determined using gel permeation chromatography (GPC). The results of the molecular weight measurements are given in Table I, and the molecular weight distribution (MWD) curves of the resins are given in Figures 1–3.

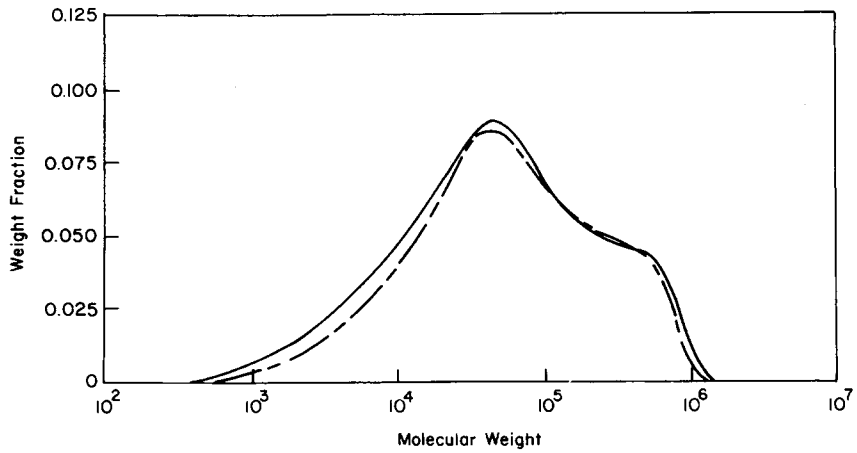

Fig. 3. Molecular weight distribution curves for Rexene Polyolefins low-density polyethylenes: (—) PE111; (- - -) PE143.

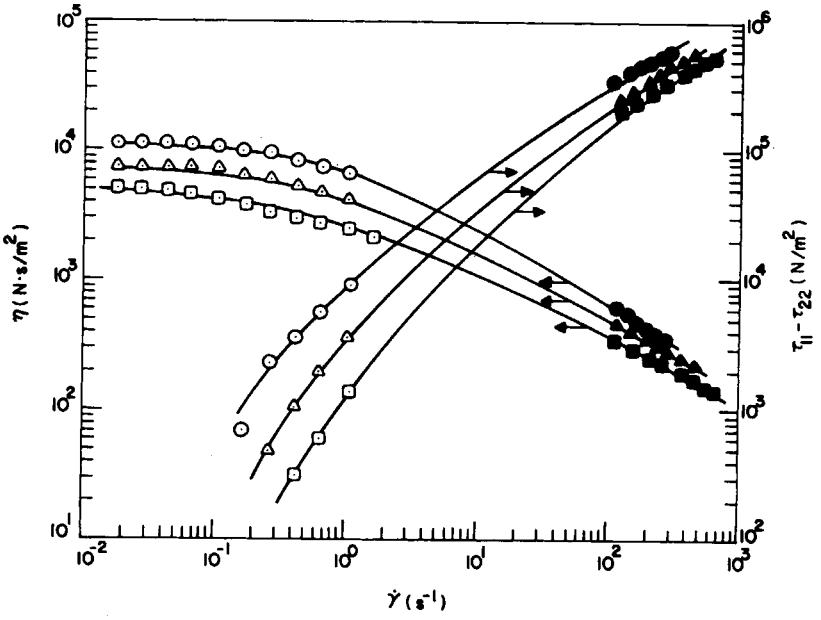

Fig. 4. η and $\tau_{11} - \tau_{22}$ vs. $\dot{\gamma}$ for Dow PE510 at various melt temperatures (°C): (⊙,●) 180; (△,▲) 200; (⊡,■) 220; (⊙,△,⊡) cone-and-plate data; (●,▲,■) capillary rheometer data.

Apparatus Employed for Rheological Measurements

Shearing Flow Apparatus. The steady shearing flow properties (both shear viscosity and first normal stress difference) were determined, using a cone-and-plate rheometer (Weissenberg rheogoniometer, Model R16) at *low* shear

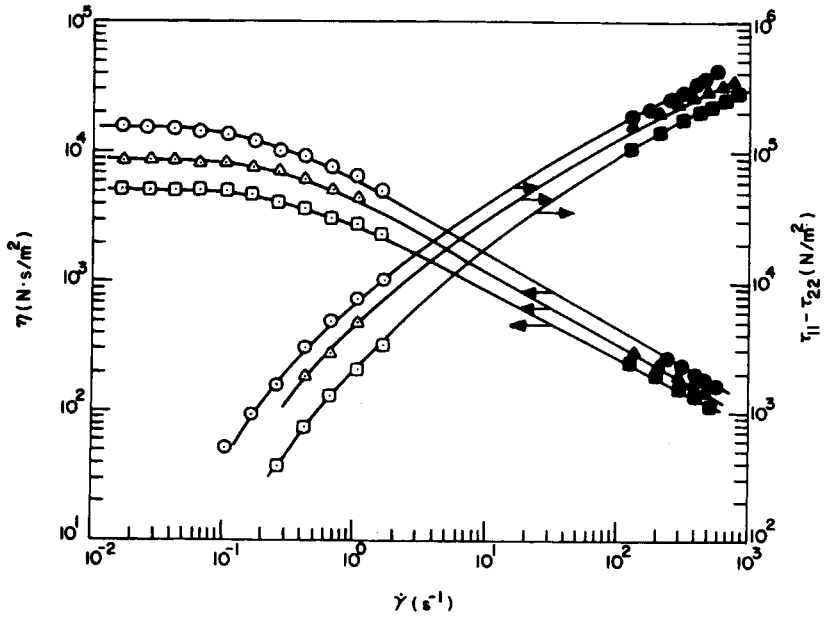

Fig. 5. η and $\tau_{11} - \tau_{22}$ vs. $\dot{\gamma}$ for Dow PE529 at various melt temperatures. Symbols are the same as in Figure 4.

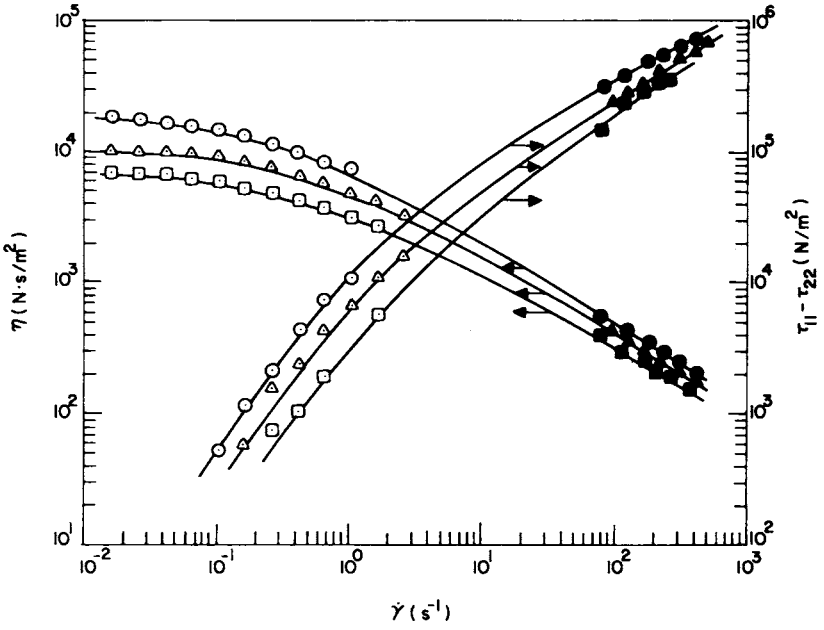

Fig. 6. η and $\tau_{11} - \tau_{22}$ vs. $\dot{\gamma}$ for Norchem PE952 at various melt temperatures. Symbols are the same as in Figure 4.

rates and a capillary rheometer at *high* shear rates. (The commercial version of this rheometer, Seiscor/Han Rheometer, is available from the Seiscor Division, Seismograph Service Corp., Tulsa, Okla.) The principles involved in the use of these rheometers are well documented in the literature.[6,7]

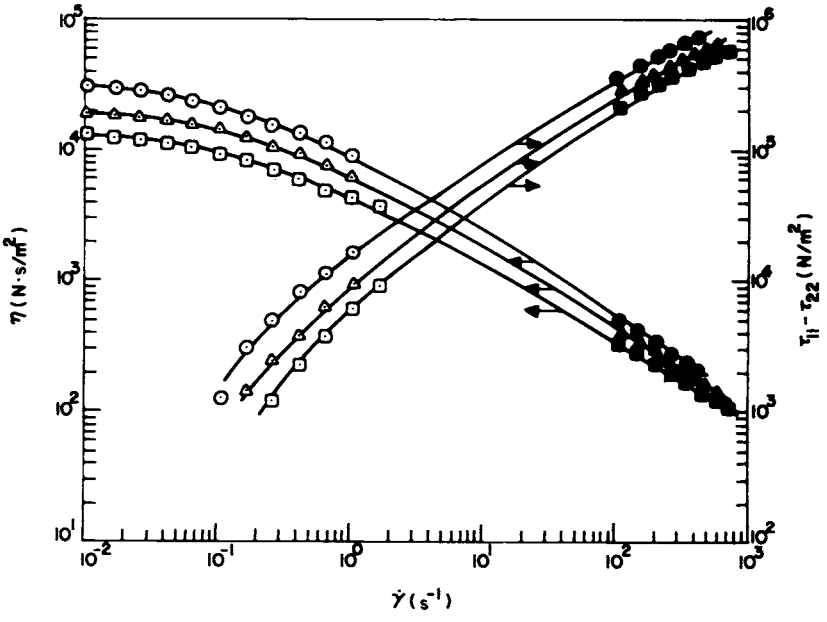

Fig. 7. η and $\tau_{11} - \tau_{22}$ vs. $\dot{\gamma}$ for Norchem PE962 at various melt temperatures. Symbols are the same as in Figure 4.

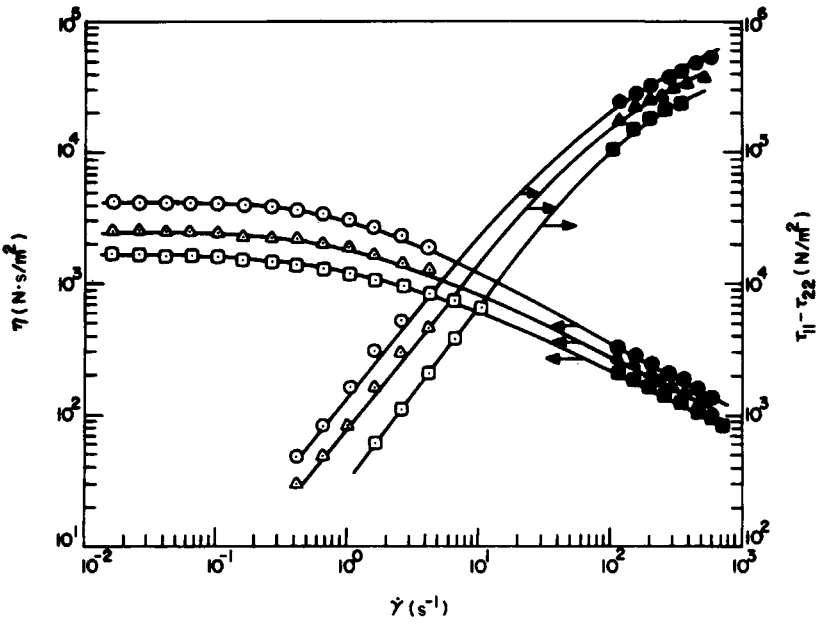

Fig. 8. η and $\tau_{11} - \tau_{22}$ vs. $\dot{\gamma}$ for Rexene PE111 at various melt temperatures. Symbols are the same as in Figure 4.

Briefly stated, the cone-and-plate rheometer employed permits one to determine the shear viscosity η and first normal stress difference $\tau_{11} - \tau_{22}$ from the following expressions:

$$\eta = \tau_{12}/\dot{\gamma} = (3\mathcal{T}/2\pi R^3)/(\Omega/\theta_c) \tag{1}$$

and

$$\tau_{11} - \tau_{22} = 2F/\pi R^2 \tag{2}$$

In eq. (1), τ_{12} denotes the shear stress, $\dot{\gamma}$ denotes the shear rate, $\mathcal{T}$ denotes the torque, R is the radius of the cone, Ω denotes the angular velocity, and θ_c is the angle formed by the cone and plate. And in eq. (2), F denotes the net thrust measured on the cone (or plate), in excess of that due to ambient pressure.

The capillary rheometer employed permits one to determine η and $\tau_{11} - \tau_{22}$ from the following expressions[7,8]:

$$\eta = \tau_w/\dot{\gamma} = [(-\partial p/\partial z)D/4]/[32Q/\pi D^3)((3n + 1)/4n)] \tag{3}$$

and

$$\tau_{11} - \tau_{22} = P_{\text{exit}} + \tau_w(dP_{\text{exit}}/d\tau_w) \tag{4}$$

In eq. (3), $(-\partial p/\partial z)$ denotes the pressure gradient, D is the capillary diameter, Q denotes the volumetric flow rate, and n is defined by

$$n = d\ \ln[(-\partial p/\partial z)D/4]/d\ \ln(32Q/\pi D^3) \tag{5}$$

And in eq. (4), P_{exit} is the wall normal stress at the die exit plane, which may be obtained by extrapolating the readings of wall normal stresses (with the aid of pressure transducers) in the fully developed region of the capillary to the exit

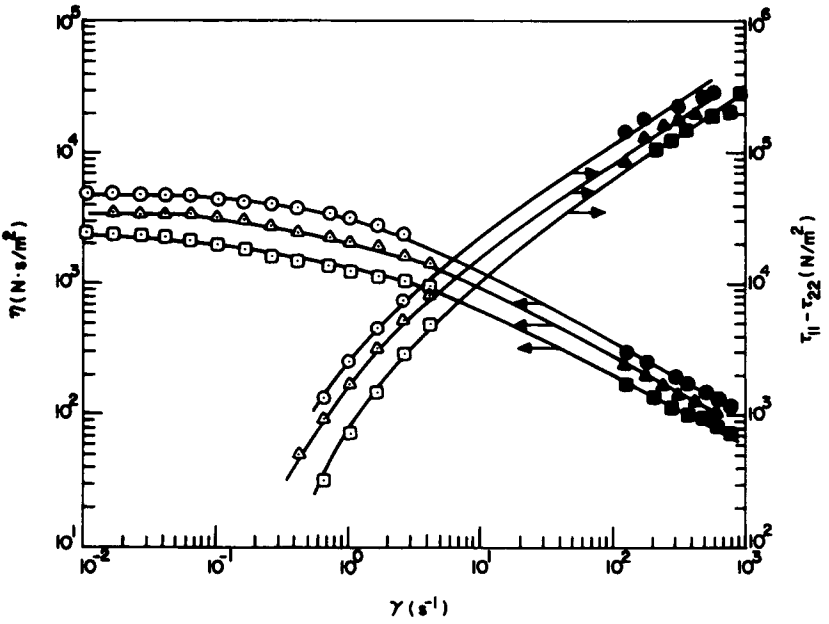

Fig. 9. η and $\tau_{11} - \tau_{22}$ vs. $\dot{\gamma}$ for Rexene PE143 at various melt temperatures. Symbols are the same as in Figure 4.

plane of the die. In the present study, a capillary having an L/D ratio of 20 (D = 3.175 mm) was used.

Elongational Flow Apparatus. The elongational viscosity was determined, using the apparatus developed by Ide and White.[9] For the experiment, filaments of about 3 mm in diameter and 30 cm long were prepared by extrusion, and they

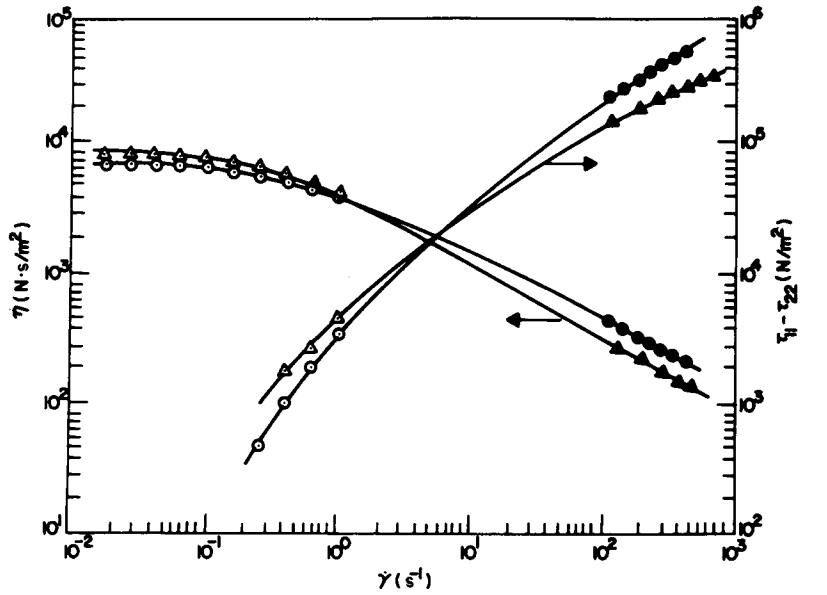

Fig. 10. η and $\tau_{11} - \tau_{22}$ vs. $\dot{\gamma}$ for Dow PE510 (⊙,●) and Dow 529 (△,▲) at 200°C.

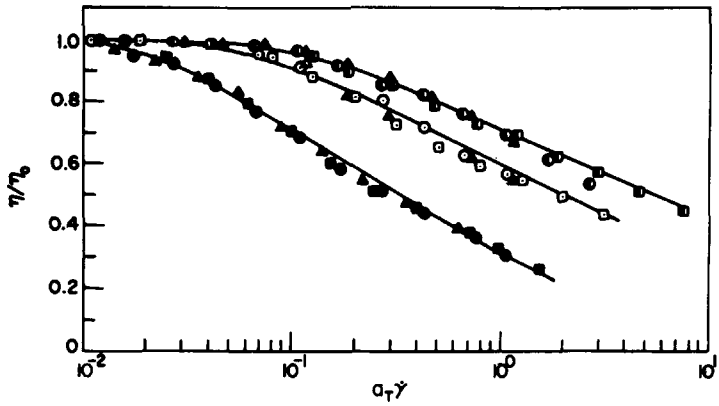

Fig. 11. η/η_0 vs. $a_T\dot{\gamma}$. (a) Dow PE510 at various melt temperatures (°C): (⊙) 180; (▲) 200; (⊡) 220. (b) Norchem PE962 at various melt temperatures (°C): (●) 180; (▲) 200; (■) 220. (c) Rexene PE111 at various melt temperatures (°C): (◐) 180; (▲) 200; (◨) 220.

were then stretched in a silicone oil bath kept at a constant temperature, applying a constant elongation rate. All experiments were carried out at 180°C, and, for each sample, three elongation rates (0.01 s^{-1}, 0.1 s^{-1}, and 1.0 s^{-1}) were applied.

Briefly stated, the elongational viscosity was calculated using the expression

$$\eta_E(t) = \frac{[F(t)/A_0]e^{(V/L)t}}{V/L} \tag{6}$$

in which $F(t)$ is the filament tension measured as a function of time t, A_0 is the initial cross-sectional area of the filament, V is the roll velocity, and L is the sample length.

RESULTS AND DISCUSSION

Melt Index and Shearing Flow Properties

Plots of viscosity η and first normal stress difference $\tau_{11} - \tau_{22}$ versus shear rate $\dot{\gamma}$ at various melt temperatures are given in Figures 4–9 for the six LDPE's employed. Note in these figures that open symbols represent the data obtained with the cone-and-plate rheometer and closed symbols represent the data obtained with the capillary rheometer. It is seen in all cases that η decreases, and $\tau_{11} - \tau_{22}$ increases, as $\dot{\gamma}$ increases, and that both η and $\tau_{11} - \tau_{22}$ decrease as melt temperature increases.

The plastics industry has long used the melt index as a rheological parameter in selecting resins for fabrication purposes. As a matter of fact, since 1965 the use of the melt index has been recommended by the American Standard Testing Method Committee (see ASTM D 1238). However, today it is a well-recognized fact that the melt index does not (and indeed cannot) describe the true rheological characteristics, responsive to the molecular characteristics, of the resin under processing conditions. We shall demonstrate below an example where the use of the melt index gives little useful information to resin fabricators.

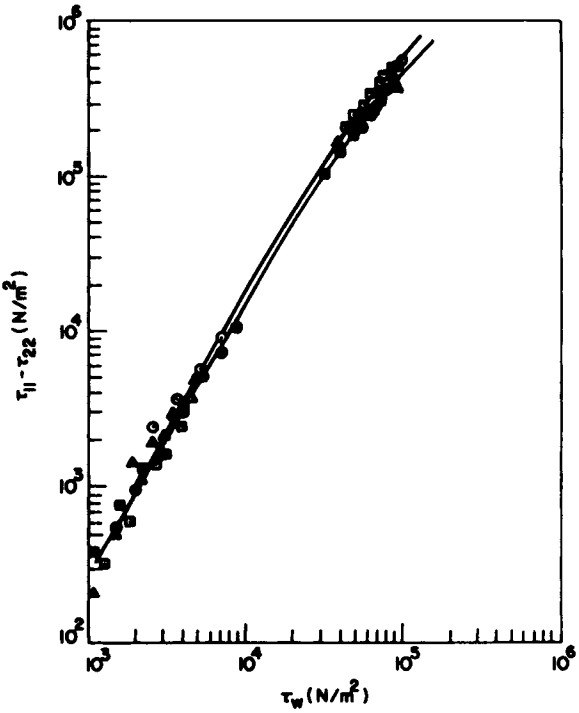

Fig. 12. $\tau_{11} - \tau_{22}$ vs. τ_w. (a) Dow PE510 at various melt temperatures (°C): (⊙) 180; (▲) 200; (⊡) 220. (b) Dow PE529 at various melt temperatures (°C): (●) 180; (▲) 200; (■) 220.

The melt index (MI) is at best a single value of viscosity at the particular shear rate (or shear stress) and temperature employed (ASTM D 1238). In view of the fact, however, that almost all the thermoplastic resins that are used in plastics fabrication processes exhibit non-Newtonian behavior, the MI is of little help in checking the quality of the resin supplied by the resin manufacturer, or in monitoring the fabrication processes, because most of the plastics fabrication operations requires processing conditions (e.g., shear rate or shear stress, melt temperature, etc.) quite different from that at which the MI is usually determined.

Moreover, not infrequently, one encounters the situation where two resins of the same molecular structure have the same value of MI, and yet quite different values of melt viscosity, not to mention melt elasticity, over a wide range of shear rates (or shear stresses). Such an example is displayed in Figure 10, in which the two resins, Dow PE510 and Dow PE529, have the same value of MI (see Table I) and are produced commercially by the same resin manufacturer. Note that the viscosity curves cross over at a shear rate of about 1.5 s^{-1}, as shown in Figure 10.

Very often, plastics fabricators are interested in controlling the shape of extrudates and/or the residual stress in injection-molded products. Such matters are little related to melt viscosity, but very much to the elastic property of the molten polymer. Melt elasticity, in turn, depends upon the processing condition (e.g., shear rate or shear stress, and melt temperature) and, also, the design of the shaping device (e.g., die, mold cavity).[7] The melt index cannot describe the elastic property of a polymer, and therefore we need to define another rheological

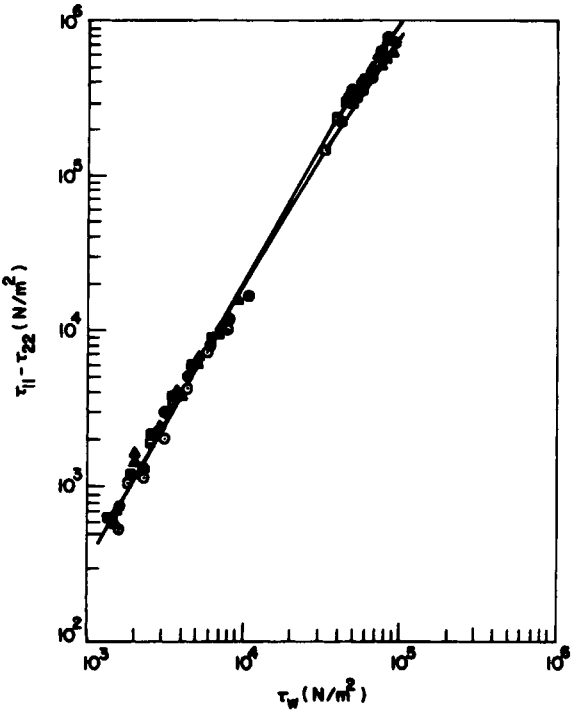

Fig. 13. $\tau_{11} - \tau_{22}$ vs. τ_w. (a) Norchem PE952 at various melt temperatures (°C): (⊙) 180; (△) 200; (⊡) 220. (b) Norchem PE962 at various melt temperatures (°C): (●) 180; (▲) 200; (■) 220.

property that will describe it. Note in Figure 10 that the two $\tau_{11} - \tau_{22}$ curves cross over at a shear rate of about 10 s^{-1}. In others words, Figure 10 shows that, at low shear rates, Dow PE510 is less elastic than Dow PE529, but at high shear rates the opposite is true.

Three facts are confirmed in Figure 10. First, the melt index does not describe the melt viscosity of a resin at the processing conditions of practical interest because the shear rates encountered in plastics processing operations of commercial interest are much higher than that used in determining it. Second, due to the fact that the melt viscosity decreases with increasing shear rate, commonly referred to as *shear-thinning* behavior, a single value of the melt viscosity at a low shear rate (i.e., the melt index) has little practical significance in predicting the melt flow behavior of a resin when subjected to practical processing conditions of commercial interest. Third, the melt index does not describe the elastic behavior of a resin.

Practical Limitations of Cone-and-Plate Rheometry

The usefulness of a cone-and-plate rheometer is limited to low shear rates, say $\dot{\gamma} < 10\ s^{-1}$, for the particular LDPE's investigated. It should be pointed out, however, that the highest value of shear rate that one can achieve with a cone-and-plate rheometer before flow instability sets in depends on the type of fluid under test. For instance, with very elastic rubbers (say, $\overline{M}_w \cong 1{,}000{,}000$) our experience indicates that the material begins to exude from the gap between the

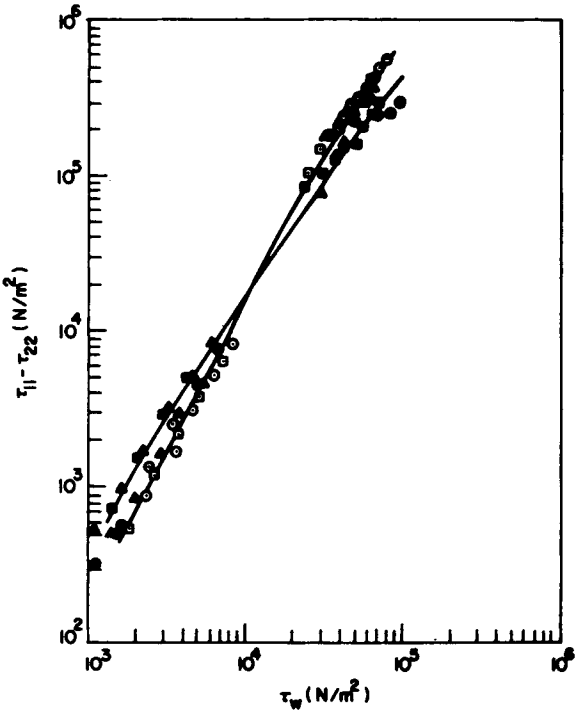

Fig. 14. $\tau_{11} - \tau_{22}$ vs. τ_w. (a) Rexene 111 at various melt temperatures (°C): (⊙) 180; (▲) 200; (⊡) 220. (b) Rexene 143 at various melt temperatures (°C): (●) 180; (▲) 200; (■) 220.

cone and plate at a shear rate of about 0.1 s^{-1}. On the other hand, when using dilute polymer solutions, one can achieve higher shear rates, say up to 1000 s^{-1}. However, as pointed out in our recent publication[10] and others,[11,12] as shear rate is increased, inertia-induced flow instability (i.e., secondary flow) sets in, again limiting the usefulness of the cone-and-plate rheometer. Note that inertia-induced flow instability gives rise to negative values of $\tau_{11} - \tau_{22}$ even for Newtonian fluids, and hence proper correction is necessary, as pointed out by Walters[6] and Kulicke et al.,[12] when dealing with viscoelastic polymer solutions.

Therefore, shear rate is not an appropriate variable for discussing the limitations of rheological instruments. Because of the differences in shear viscosity, for instance, between typical thermoplastic resins and elastomers, the ranges of shear rates involved in processing such materials are quite different. However, when using shear stress instead of shear rate, the range of shear stresses involved becomes independent of the type of materials that one may be processing. Therefore, shear stress must be used in discussing the limitations of rheological instruments. As will be shown below, the highest shear stress at which a cone-and-plate rheometer can generate reliable rheological information is in the neighborhood of 10^4 N/m^2. Such values of shear stress are far too low to be meaningful in *many* polymer processing operations.

Temperature-Independent Correlation of Shearing Flow Properties

Figure 11 gives plots of η/η_0 vs. $a_T\dot{\gamma}$ for the three resins, Rexene PE111, Dow PE510, and Norchem PE962, in which η_0 is the zero-shear viscosity and a_T is

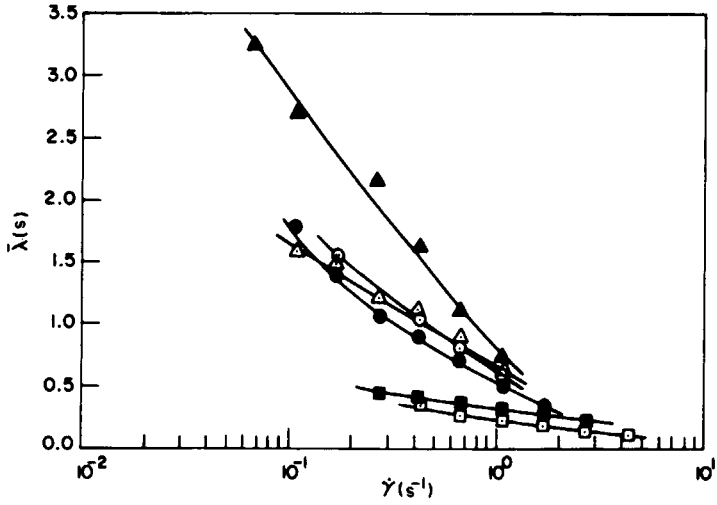

Fig. 15. $\bar{\lambda}$ vs. $\dot{\gamma}$ at 180°C: (⊙) Dow PE510; (●) Dow PE529; (△) Norchem PE952; (▲) Norchem PE962; (⊡) Rexene PE111; (■) Rexene PE143.

an empirical shift factor. Note that a_T is obtained by shifting the viscosity data at various temperatures to a reference temperature (180°C in the present case). In other words, we have obtained a temperature-independent correlation of viscosity curves in terms of η/η_0 and $a_T\dot{\gamma}$. Similar results have very recently been reported.[13]

Figure 12 gives plots of $\tau_{11} - \tau_{22}$ vs. τ_w for Dow PE510 and Dow PE529, in which values of $\tau_{11} - \tau_{22}$ were obtained at low shear stresses (up to 10^4 N/m^2)

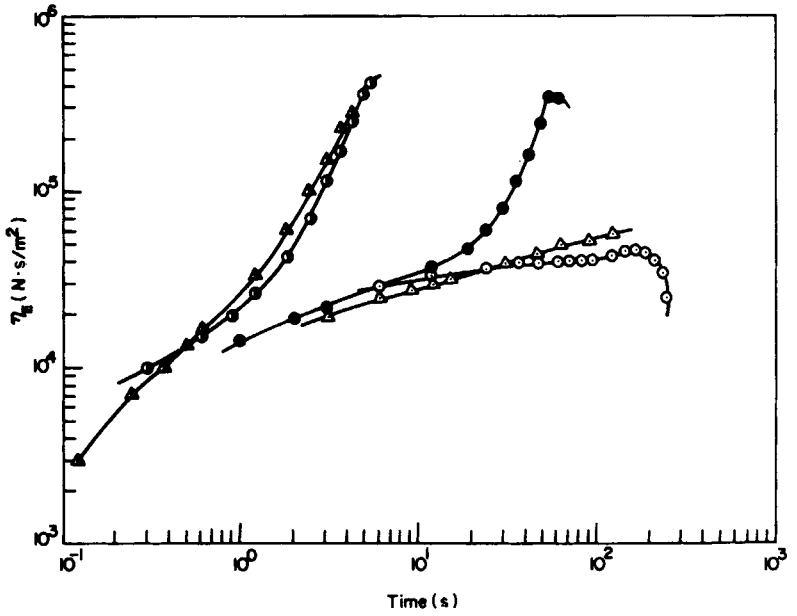

Fig. 16. η_E vs. time at 180°C. (a) Dow PE510 at various values of constant elongation rate (s^{-1}): (⊙) 0.01; (●) 0.10; (◑) 1.00. (b) Dow PE529 at various values of constant elongation rate (s^{-1}): (△) 0.01; (▲) 1.00.

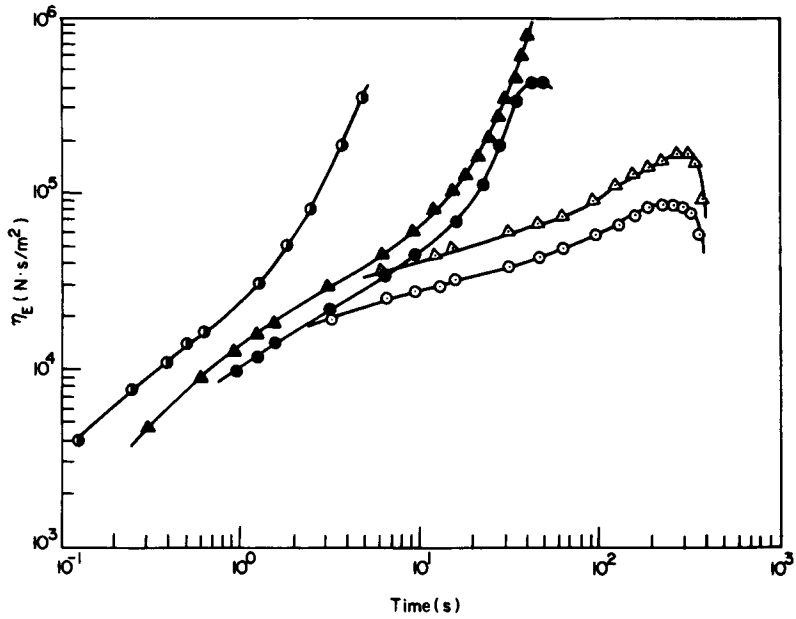

Fig. 17. η_E vs. time at 180°C. (a) Norchem PE952 at various values of constant elongation rate (s^{-1}): (⊙) 0.01; (●) 0.10; (◑) 1.00. (b) Norchem PE962 at various values of constant elongation rate (s^{-1}): (△) 0.01; (▲) 0.10.

with the cone-and-plate rheometer and at high shear stresses ($4 \times 10^4 - 1.5 \times 10^5$ N/m^2) with the capillary rheometer. Note in this figure that $\tau_{11} - \tau_{22}$ correlates very well with τ_w, independent of temperature. Such an observation was first reported earlier by Han and co-workers[7,14–16] and later by White and co-workers.[17] It is of interest to observe in Figure 12 that the two resins, Dow PE510 and Dow PE529, have essentially the same degree of melt elasticity at low shear stresses, as determined by the cone-and-plate rheometer, and that the difference in melt elasticity between the two resins becomes noticeable only as the shear stress is increased beyond the value at which the cone-and-plate rheometer loses effectiveness. It is clear in Figure 12 that, at high shear stresses, Dow PE510 is more elastic than Dow PE529.

Figure 13 gives plots of $\tau_{11} - \tau_{22}$ vs. τ_w for Norchem PE952 and Norchem PE962. It is seen that very little difference in melt elasticity exists between the two resins at low shear stresses (up to 1.5×10^4 N/m^2), and that a noticeable difference is seen at high shear stresses, with Norchem PE952 more elastic than Norchem PE962.

Figure 14 gives plots of $\tau_{22} - \tau_{22}$ vs. τ_w for Rexene PE111 and Rexene PE143. It is seen that at low shear stresses Rexene PE143 is more elastic than Rexene 111 and that at high shear stresses the opposite is true.

Effects of the Molecular Weight Distribution on Shearing Flow Properties

It may be observed from Figure 11 that the broader the molecular weight distribution (MWD) (see Table I), the greater the shear-thinning behavior of

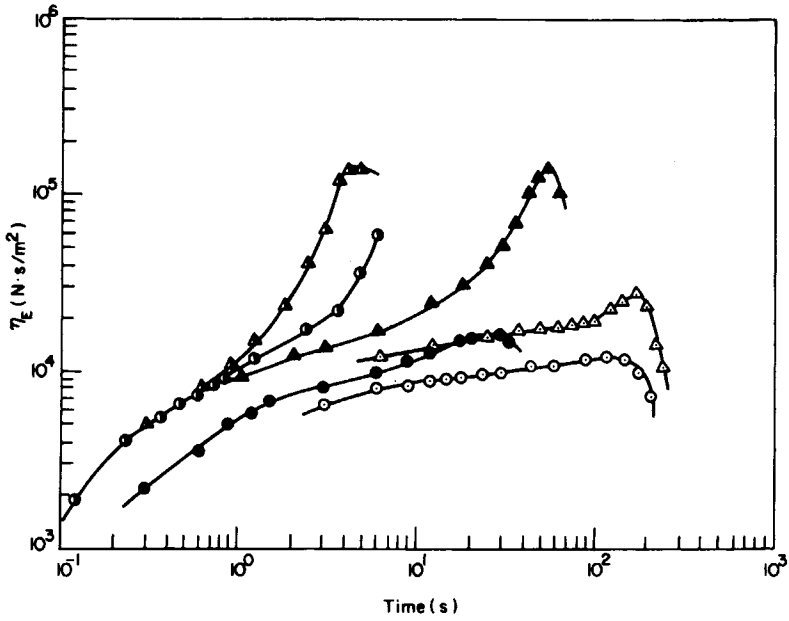

Fig. 18. η_E vs. time at 180°C. (a) Rexene PE111 at various values of constant elongation rate (s^{-1}): (⊙) 0.01; (●) 0.10; (◑) 1.00. (b) Rexene PE143 at various values of constant elongation rate (s^{-1}): (△) 0.01; (▲) 0.10; (▲) 1.00.

the resin (i.e., the more rapidly the viscosity decreases as the shear rate increases). The values of the power-law constant n in the expression

$$\eta = K\dot{\gamma}^{n-1} \tag{7}$$

are 0.46 for Rexene PE111, 0.42 for Dow PE510, and 0.37 for Norchem PE962.

In view of the fact that the shear-thinning behavior of polymeric liquids is attributable to the disentanglement of macromolecules under a shearing motion, the results shown in Figure 11 seems to indicate that the broad MWD polymer may be disentangled much more readily than the narrow MWD polymer.

Figure 15 gives plots of characteristic time $\bar{\lambda}$ vs. shear rate $\dot{\gamma}$ for the six resins, in which $\bar{\lambda}$ is defined as

$$\bar{\lambda}(\dot{\gamma}) = (\tau_{11} - \tau_{22})/2\eta\dot{\gamma}^2 \tag{8}$$

A trend is seen in Figure 15 that the broad MWD resin has higher values of $\bar{\lambda}$ than does the narrow MWD resin, and that $\bar{\lambda}$ falls off more rapidly as the MWD broadens (see Table I). Since $\bar{\lambda}$ may be interpreted as representing the elastic behavior of polymeric liquids, the results shown in Figure 15 seem to indicate that the broad MWD polymer is more elastic than the narrow MWD polymer.

Elongational Flow Behavior

Figure 16 gives plots of elongational viscosity η_E vs. time t for Dow PE510 and Dow PE529. Similar plots are given in Figure 17 for Norchem PE952 and Norchem PE962, and in Figure 18 for Rexene PE111 and Rexene PE143. It is

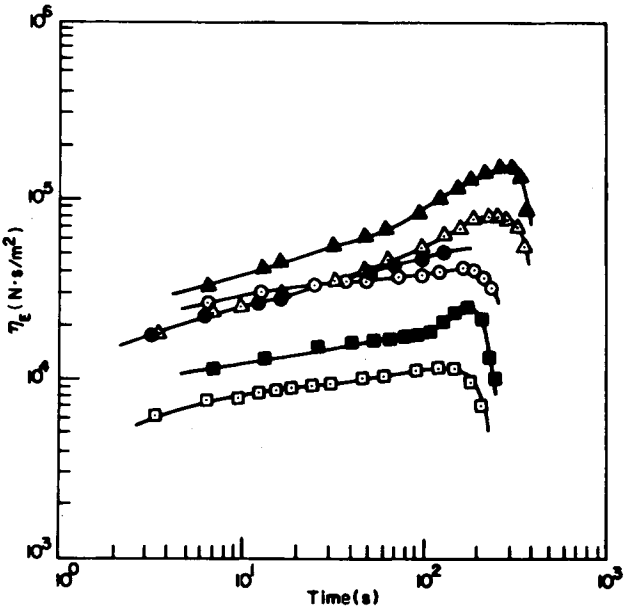

Fig. 19. η_E vs. time at $\dot{\gamma}_E = 0.01\ s^{-1}$: (⊙) Dow PE510; (●) Dow PE529; (△) Norchem PE952; (▲) Norchem PE962; (⊡) Rexene PE111; (■) Rexene PE143.

seen in these figures that a steady state elongational viscosity was approached only at low elongation rates.

Figure 19 gives plots of elongational viscosity η_E vs. time t for the six resins, at elongation rate $\dot{\gamma}_E = 0.01\ s^{-1}$. It is seen that η_E attains steady state values, except for Dow PE529. Note in Table I that the MWD's of the two resins from the same resin manufacturer are much closer than the MWD's of the resins from different resin manufacturers. For this reason, and also in order to facilitate

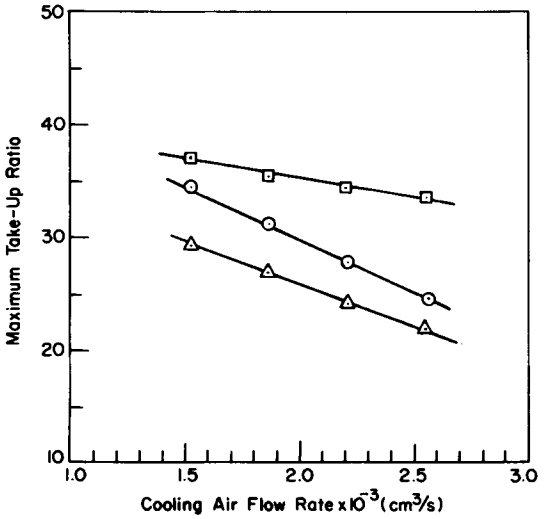

Fig. 20. Maximum takeup ratio vs. cooling air flow rate at a blowup ratio of 3.5: (⊡) Rexene PE143; (⊙) Dow PE 510; (△) Norchem PE952.

our discussion below, let us consider the elongational viscosities of three resins, Dow PE510, Norchem PE952, and Rexene PE143, one from each resin manufacturer. It is seen in Figure 19 that Rexene PE143 has the lowest η_E of the three resins under consideration, i.e.,

$$(\eta_E)_{\text{Rexene 143}} < (\eta_E)_{\text{Dow 510}} < (\eta_E)_{\text{Norchem 952}} \tag{9}$$

Referring to Table I, the breadth of MWD of the three resins has the following ordering:

$$(\text{MWD})_{\text{Rexene 143}} < (\text{MWD})_{\text{Dow 510}} < (\text{MWD})_{\text{Norchem 952}} \tag{10}$$

It appears from inequalities (9) and (10) that the elongational viscosity increases as the molecular weight distribution broadens. It is worth mentioning at this juncture that such a correlation was reported earlier by Han and Lamonte,[18] who conducted a melt spinning study. More recently, Minoshima et al.[19] reported that, over the range of elongation rate $\dot{\gamma}_E$ investigated, the elongational viscosity η_E of the broad MWD polypropylene resins decreased with increasing $\dot{\gamma}_E$, whereas the η_E of the narrow MWD polypropylene resins increased with $\dot{\gamma}_E$.

Using the same resins referred to above in Figure 19, we have also conducted a series of film blowing experiment. The details of the experimental apparatus and procedure employed are described elsewhere.[20] Of the experiments conducted, one, which is relevant to our discussion here, was to determine the maximum takeup ratio (TUR) by increasing the takeup speed slowly until the tubular bubble broke, while maintaining the other processing conditions constant. The results of the experiment are summarized in Figure 20. It is seen in Figure 20 that the maximum TUR of the resins studied follows the sequence

$$\text{Rexene PE143} > \text{Dow PE 510} > \text{Norchem PE952} \tag{11}$$

If we regard the maximum TUR as a measure of tubular film blowability, we can conclude that, of the three resins employed, Rexene PE143 has the best blowability.

In view of the fact that tubular film blowing involves elongational flow, one may surmise that the tubular film blowability of a resin might be correlatable to its elongational viscosity. A close look at inequalities (9) and (11) seems to indicate that the resin having the lower elongational viscosity does indeed have better tubular film blowability. This observation is consistent with that reported earlier by Han and co-workers,[18,21] who investigated the spinnability of various thermoplastic resins in melt spinning operations.

We wish to acknowledge that Professor James L. White at the University of Tennessee allowed us to use the elongational rheometer in his laboratory.

References

1. E. B. Bagley, *J. Appl. Phys.*, **31**, 1126 (1960).
2. J. E. Guillet, R. L. Combs, D. F. Slonaker, D. A. Weems, and H. W. Coover, *J. Appl. Polym. Sci.*, **9**, 757 (1965).
3. R. L. Combs, D. F. Slonaker, and H. W. Coover, *J. Appl. Polym. Sci.*, **13**, 519 (1969).
4. L. Wild, R. Ranganath, and D. C. Knobelock, *Polym. Eng. Sci.*, **16**, 811 (1976).
5. C. D. Han and C. A. Villamizar, *J. Appl. Polym. Sci.*, **22**, 1677 (1978).

6. K. Walters, *Rheometry*, Chapman and Hall, London, 1975.
7. C. D. Han, *Rheology in Polymer Processing*, Academic, New York, 1976.
8. C. D. Han, *Trans. Soc. Rheol.*, **18,** 163 (1974).
9. Y. Ide and J. L. White, *J. Appl. Polym. Sci.*, **22,** 1061 (1978).
10. K. W. Lem and C. D. Han, paper presented at the Annual Meeting of the Society of Rheology, Louisville, Ky., October 1981; *J. Rheol.*, **27,** 263 (1983).
11. R. G. King, *Rheol. Acta*, **4,** 265 (1965).
12. W. M. Kulicke, G. Kiss, and R. S. Porter, *Rheol. Acta*, **16,** 568 (1977).
13. K. W. Lem and C. D. Han, *J. Appl. Polym. Sci.*, **27,** 1367 (1982).
14. C. D. Han and Y. W. Kim, *Trans. Soc. Rheol.*, **19,** 245 (1975).
15. C. D. Han and K. W. Lem, *Polym. Eng. Rev.*, **2,** 135 (1982).
16. C. D. Han and D. A. Rao, *J. Appl. Polym. Sci.*, **23,** 225 (1979).
17. K. Oda, J. L. White, and E. S. Clark, *Polym. Eng. Sci.*, **18,** 25 (1978).
18. C. D. Han and R. R. Lamonte, *Trans. Soc. Rheol.*, **16,** 447 (1972).
19. W. Minoshima, J. L. White, and J. E. Spruiell, *Polym. Eng. Sci.*, **20,** 1166 (1980).
20. C. D. Han and T. H. Kwack, *J. Appl. Polym. Sci.*, **28,** 3399 (1983).
21. C. D. Han and Y. W. Kim, *J. Appl. Polym. Sci.*, **18,** 2589 (1974).

Received January 27, 1983
Accepted May 20, 1983